Quantifying the value of flexibility: demand response versus storage

Wim van Ackooij[a], Ana P. Chorobura[b,1,*], Claudia Sagastizábal[c,2], Hasnaa Zidani[d]

[a] *EDF R&D, OSIRIS Department, 7 Boulevard Gaspard Monge, 91120 Palaiseau, France*
[b] *Federal University of Paraná, Graduate Program in Mathematics, CP 19081, CEP 81531-980, Curitiba-Brazil*
[c] *Institute of Mathematics, Statistics, and Scientific Computing, State University of Campinas (IMECC - UNICAMP), Rua Sérgio Buarque de Holanda 651, 13083-859, Campinas, SP, Brazil.*
[d] *Unité de Mathématiques Appliquées (UMA), Ensta ParisTech, 828 Bd des Maréchaux, 91762 Palaiseau Cedex*

Abstract

Intermittent sources of energy represent a challenge for electrical networks, particularly regarding demand satisfaction at peak times. Energy management tools such as load shaving or storage systems can be used to mitigate abrupt variations in the network. The value of different mechanisms to move energy through time is determined by a multi-objective programming approach, that aims at minimizing operating costs as well as carbon emissions. By combining the output with sensitivity theory, the new technique builds a three-dimensional Pareto front, in which the usual information on indifference costs is accompanied by a third dimension that provides the decision maker with a quantitative measure to evaluate the relative impact of the two conflicting objectives. The interest of the methodology is assessed on three instances representing typical configurations in Brazil, Germany and France, respectively corresponding to a system that is hydro-dominated, thermo-dominated, and with a balanced mix of hydro and thermal power.

Keywords: Multi-objective programming, Energy management tools, Sensitivity analysis.

1. Introduction

Electricity systems must have enough generation capacity to satisfy the network load at every time step. As energy consumption varies greatly -along a given day or a given month-, ensuring that there is enough power in the grid at peak times is a challenging issue, e.g., [1]. For many years, hydro-reservoirs played the fundamental role of storages, allowing to move energy along time without much waste for the system. To achieve a sound management of hydro-energy in such a context, the *value* given to water via the *future cost function*, typically obtained by the stochastic dual dynamic programming approach [2] was and remains fundamental.

In the last years, sustainability concerns accelerated the penetration of green technologies, adding a new layer of complexity to the problem. Like the water inflows, the sun and winds are available to the system in uncertain amounts and at times not known in advance. Unlike water, however, those other sources of energy are not directly coupled with a storage device like a reservoir. Without storage devices to mitigate the intermittent nature of solar and wind power, any generated energy that is not consumed immediately is simply lost. Moreover, since the system is operated in an economical manner, if at a given time, the uncertain (cheap) green power is planned to be injected in the network, then (expensive) thermal units are not turned on. In real time, however, it may happen that at a later time, say a peak hour, the realization of green energy is less than expected. In this situation, not to shed the load, more thermal generation is needed, to compensate for the lack of power. However, because of ramping constraints, units that are off and have slow dynamics cannot be turned on in time. For this reason (very expensive and highly polluting) thermal units, with fast dynamics, may need to be dispatched. The question that arises naturally in this setting is

what is the value of green energy,
in terms of the power system as a whole?

A complete answer to this question would require to create a future cost function for wind power. Since there are no wind storages, the value that this type of energy

*Corresponding author
Email addresses: wim.van-ackooij@edf.fr (Wim van Ackooij), ana.chorobura@gmail.com (Ana P. Chorobura), sagastiz@unicamp.br (Claudia Sagastizábal), hasnaa.zidani@ensta-paristech.fr (Hasnaa Zidani)

[1] Research supported by Capes-Brazil and PGMO.
[2] Research supported by CNPq Grant 303905/2015-8.

brings to the system system must be computed in a different manner. This work addresses the issue in an indirect manner, by quantifying the impact of moving energy along time. We consider the same power system operating under three different premises, namely,

- a base case, with no mechanism put in place,
- the same system, with a demand-response tool to "shave" the load, and
- the same system, endowed with batteries to store energy.

Demand-side management tools, more precisely load shaving, can be used to mitigate abrupt changes in the generation. Another tool is to rely on virtual entities, representing a group of small generators coupled with a battery. The latter is a good alternative to store eventual over-production of energy, that can be supplied to the system at peak times, when there is a shortage of generation. The battery functions as a reservoir that can be depleted when most needed. This storage is not free, as some energy is lost when charging and discharging the battery.

Since sustainability is an important goal, our valuation process takes into account not only cost minimization but also environmental impact, seen through a CO2 criterion. Based on [3], we incorporate in the model as second objective the minimization of the carbon emission of the thermal units in the system.

In multi-objective optimization it is well-known that all the criteria cannot be minimized simultaneously, and that a trade-off is given by the Pareto front. For our problem of interest, Pareto points are combinations of (minimum) operating costs and carbon emissions of the thermal plants that are "the same": no objective can be reduced without making the other one worse. The bi-objective programming approach is put in place by means of a Chebyshev scalarization [4–6].

Under the zero carbon emission paradigm that is now guiding the configuration of future power systems, it is useful to get an additional indicator for the Pareto points. Specifically, we add a *third dimension* to the bi-dimensional Pareto front, with the sensitivity of operating costs with respect to variations on the carbon emissions. The new information, akin to the well-known shadow prices in Linear Programming, provides the decision maker with a quantitative measure to evaluate the relative impact of variations of the two conflicting objectives and gives an additional measure of the value of green technologies for the system.

The calculation of the new third dimension relies on sensitivity theory, see Theorem 2. It turns out that is possible to derive the sensitivity indicator without solving any additional problem, directly from the bi-objective programming solution.

The interest of the methodology is assessed on three instances representing typical configurations in Brazil, France and Germany, The Brazilian electricity generation matrix is hydro-dominated. As the investment required to build new hydro-electric plants is too large, in the last years the power mix has noticeably increased the proportion of thermal power plants. The French system is balanced in terms of sources of energy. In Germany, most of the power generated from conventional sources (not from wind or sun), is of thermal origin.

This work is organized as follows. In Section 2 we describe the considered generation assets. Section 3 presents the load shaving mechanism and the battery dynamics. In section 4 we summarize the three configurations of the bi-objective optimization problem: the base case, the problem with load-shaving and the problem with a battery. Section 5 discusses concepts, properties and solution method for bi-objective optimization problems. This section contains the new sensitivity result. In Section 6, the numerical results are presented and analyzed. Section 7 concludes the paper with final remarks.

2. Specification of the power system

After fixing some notation in the nomenclature below, we describe the set of thermal, hydro, solar and wind plants used to generate electricity. Thermal units are modelled as in economic dispatch problems. For a complete account of trends in unit-commitment we refer to [7, 8]. Let us also refer to [9] for a deep discussion on cascaded reservoir management.

The time horizon consists of T homogenously spaced time steps, each one of h hours.

Nomenclature

δ^t	Displaced energy at time t
γ	Bound for the power that can be shifted along the planning horizon
ν^t	Maximum power that can be displaced at time t
ρ_i	Turbining efficiency of turbine i at time t
ρ_I, ρ_O	Efficiency ratios for the charge and discharge processes of the battery, respectively

θ_j Gradient of thermal unit j related to the ramping constraint

b_I^t, b_O^t Input and output power of the battery at time t, respectively

b_I^{max}, b_O^{max} Maximum input and output of the battery, respectively

c_j Generation cost of thermal unit j

c_{w_k} Value of the water of reservoir k

$D_{n,k}^d n$, $D_{n,k}^u p$ Downhill and uphill flow delay, respectively

f_j Fuel emission of thermal unit j

h Time step

I_k^t Natural inflow of reservoir k at time t

K Number of reservoirs

N Number of thermal units

p_j^t Power generated by thermal unit j at time t

Q_B Maximum capacity of the battery

q_i^t flow rate of turbine i at time t

q_i^{min}, q_i^{max} Bounds of flow rate of turbine i

T Number of time steps

U^t sum of the energy generated by solar, run-of-the-river and wind thermal units at time t

V_k^t Water level of reservoir k at time t

V_k^{min}, V_k^{max} Volumetric bounds of reservoir k

y^t State of charge of the battery at time t

y^{min}, y^{max} Bounds of the state of the charge

z_k^t Amount of water available to generate power in the reservoir k at time t

2.1. Power assets in the system

Since our interest is in computing the Pareto efficient frontier, the model was simplified, so that there are no 0-1 variables (as in economic dispatch problems). Typically, solving bi-objective optimization problems requires the iterative solution of many subproblems, which would be (excessively) time consuming otherwise. The framework remains nonetheless compatible with a system setting involving binary variables.

2.1.1. Thermal units

A thermal unit j has an output level p_j^t in megawatts (MW) at a given proportional cost c_j in e.g., €/ MWh. If the system has N thermal units, the total operating cost is:

$$\sum_{t=1}^{T}\sum_{j=1}^{N} c_j p_j^t h\,. \tag{1}$$

Convex quadratic costs can be incorporated in the model, if desired.

To control the carbon emission f_j that results from burning fuel to generate thermal power, we extend the approach in [3]. The objective is to minimize the worst-case CO_2 emissions (tonnes/MWh), over time. Accordingly, the second objective function is given by

$$\max\left\{\frac{1}{L^t}\sum_{j=1}^{N} f_j p_j^t : t = 1,\ldots,T\right\} \tag{2}$$

where L^t denotes the demand at time step t. The worst-case criterion, of a maximum along time steps instead of a sum, yields a better control of emissions, while still allowing for a certain amount of CO_2 emission over the planning period.

For thermal units, technological constraints refer to *capacity bounds*

$$0 \le p_j^t \le p_j^{max}, \qquad t = 1,\ldots,T, \tag{3}$$

where p_j^{max} is the maximum generation capacity of thermal unit j: and *ramping constraints* limiting power variation between two consecutive time steps:

$$-\theta_j h \le p_j^t - p_j^{t-1} \le \theta_j h, \qquad t = 1,\ldots,T. \tag{4}$$

The initial power level p_j^0, for $j = 1,\ldots,N$, is given and the ramping rate θ_j is considered constant.

2.1.2. Hydro power plants with cascaded reservoirs

The considered hydro power plants are distributed along a hydro valley. This is a set K of reservoirs connected through turbines that can be used to generate electricity. We assume that each reservoir k, disposes of a set of uphill reservoirs $A(k)$ and a set of downhill reservoirs $B(k)$. Associated with each connection between reservoirs m and k is an uphill and downhill flow delay $D_{m,k}^{up}$, $D_{m,k}^{dn}$ as well as a turbining station. Moreover each reservoir disposes of natural inflows I_k^t (m^3/h) as well as two volumetric bounds V_k^{min}, V_k^{max}. For reservoirs m, k we associate with the arc (m, k) the set of turbines $\mathcal{T}_m^k$. With each turbine $i \in \cup\mathcal{T}_m^k$ we associate a flow rate q_i^t (m^3/h) and turbining efficiency ρ_i^t (MWh/m^3).

Since water is naturally free, and not attributing it a value would lead to premature depletion of this resource, c_{w_k} in ($€/m^3$) represents the cost of the water of each reservoir k. We refer to [10] for an extensive discussion on how this value of water can be computed, including the future cost function from [2]. Denote by V_k^t the water level of each reservoir at time t. The initial volume V_k^0 is known in advance, so we define $z_k^0 = V_k^0 - V_k^{min}$ indicating the amount of water available for generating power at the initial time. We also introduce variables $z_k^T = V_k^T - V_k^{min}$ indicating for each reservoir k the amount of water available for generating power at the final time. Then, the value of the final water level to be minimized in the cascaded reservoir system is equal to:

$$\sum_{k=1}^{K} c_{w_k}(z_k^0 - z_k^T) = \sum_{k=1}^{K} c_{w_k}(V_k^0 - V_k^T). \tag{5}$$

The water balance equation is

$$\begin{aligned} V_k^t = V_k^{t-1} + I_k^t h + \sum_{m\in A(k)} \sum_{i\in\mathcal{T}_k^m)} q_i^{t-D_{m,k}^{dn}} h \\ - \sum_{m\in B(k)} \sum_{i\in\mathcal{T}_k^m} q_i^{t-D_{k,m}^{up}} h, \\ \text{for } t = 1,\dots,T,\ k = 1,\dots,K \end{aligned} \tag{6}$$

with related constraints given below, for the volumes:

$$\begin{aligned} & V_k^{min} \le V_k^t \le V_k^{max} && t = 1,\dots,T,\ k = 1,\dots,K \\ & z_k^T = V_k^T - V_k^0 && k = 1,\dots,K \\ & 0 \le z_k^T \le V_k^{max} - V_k^{min} && k = 1,\dots,K \end{aligned} \tag{7}$$

and the outflows

$$q_i^{min} \le q_i^t \le q_i^{max}, \quad i \in \bigcup_{(m,k)} \mathcal{T}_k^m,\ t = 1,\dots,T. \tag{8}$$

Finally, the generated hydro-power at time t is

$$\sum_{(m,k)} \sum_{i\in\mathcal{T}_k^m} \rho_i^t q_i^t.$$

2.1.3. Solar, wind and run-of-the-river plants

Photovoltaic panels, wind turbines and run-of-the-river hydro plants generate electricity at no cost, but the generation pattern cannot be controlled. In our simplified model, we consider this to be given deterministic data. Hence, the corresponding generation U^t in MW at time t, the sum of solar, wind and run-of-the-river power, is substracted from the demand.

3. Tools to move energy through time

We compare two mechanisms to smooth peaks in the load, one is demand-side management and the other one the use of batteries. A review of different strategies for peak load shaving is presented in [11]; see also [12]. The benefits and challenges of the mechanism for the UK grid are discussed in [13]. A study involving domestic hot water systems can be found in [14].

Batteries employed as storage devices are considered in [15] The work [16] studies the use of batteries to eliminate the peaks and valleys in the load profile. In addition to improving the voltage profile at peak hours, the authors show a battery reduces the load and the system losses. A multi-objective approach to batteries can be found in [17], where the objectives considered are the reliability and economy by choosing optimal energy storage parameters subject to the constraints for a specific distribution system. For the impact of batteries from the consumer point of view, we refer to [18].

3.1. Load shaving

Load shaving, or more generally demand-side management, is related to some incentive to displace a portion of the electrical consumption from one moment in time to another one, when the system is less stressed. Typical examples of consumption that can be moved in time are charging an electrical vehicle, or using a dishwasher. The idea is to program a shift in time of such use of electricity, under some constraints. The advantage of disposing of such a tool stems from the removing electrical use away from peaking hours to off-peak hours, where the same energy can be produced using cheaper technologies. Although the literature discusses, seemingly, different variants under various names (peak shaving, valley filling, load shifting), they are essentially and mathematically the same object. Namely, a mechanism designed to move load along time, in a manner that demand remains satisfied. One could argue that some of these shifts are not of zero sum, when total energy consumption is taken into account. Indeed, one can think of rebound effects (say, requiring additional energy to heat a room when temperature has fallen too much). Incorporating such features involves binary variables, which would over-complexify the Pareto problems. Instead, the following simpler model, with energy neutral shift, is considered:

$$\begin{aligned} & -\gamma \le \delta^t \le \nu^t \le \gamma, && t = 1,\dots,T, \\ & \nu^t \ge 0 && t = 1,\dots,T, \\ & \sum_0^T \delta^t h = 0,\ \sum_0^T \nu^t h \le \gamma, \end{aligned} \tag{9}$$

where δ^t is the displaced energy at time step t, v^t is the maximum power that can be displaced at each period and γ is a bound for the power, in megawatts, that can be shifted along the planning horizon.

3.2. Batteries as storage systems

The battery, modelled as in [3, 19], can store energy for later use, but has limited capacity and power. Moreover the storage is not free, as some energy is lost when charging and discharging the battery. The level of power in the battery defines the state of the system.

Given a initial battery level, the state y^0, the dynamic evolution of the battery state of the charge y is given by the equations

$$y^{t+1} = y^t + \frac{h}{Q_B}(b_I^t \rho_I - \frac{b_O^t}{\rho_O}), \quad \text{for all } t = 1, \dots, T, \tag{10}$$

where Q_B is the maximum battery capacity, $b_I^t,\ b_O^t > 0$ are the input and output power, and $\rho_I,\ \rho_O \in [0, 1]$ are the efficiency ratios for the charge and discharge processes, assumed constant. Also, for physical reasons, variables are bounded:

$$\begin{array}{ll} y^t \in [y^{min}, y^{max}], & \text{for all } t = 1, \dots, T, \\ b_I^t \in [0, b_I^{max}], & \text{for all } t = 1, \dots, T, \\ b_O^t \in [0, b_O^{max}]., & \text{for all } t = 1, \dots, T. \end{array} \tag{11}$$

Typically, batteries have a short storage cycle and a cost of operation is not necessarily attributed to it. To handle this issue in a day to day operation, a possible, rather natural condition, is to assume that the cycle balances off over the considered time frame. This is translated into the constraint that the final storage level should be at least as favourable as the initial one:

$$y^T \geq y^0. \tag{12}$$

4. Three bi-objective optimization problems

For the analysis we have in mind, the performance of the same power system is considered when no tool for moving energy through time is implemented, when a load shaving mechanism is applied, and when the system is endowed with a battery. In the three instances, the first objective refers to the cost of operating thermal units and the "cost" of water, as in (1) and (5). The second objective measures the maximum amount of carbon emissions of thermal units, along the time horizon, as in (2). Accordingly,

$$J(p, z) := \left(\sum_{j=1}^{N} \sum_{t=1}^{T} c_j^t p_j^t h + \sum_{k=1}^{K} c_{w_k}(z_k^0 - z_k^T), \right. \\ \left. \max \left\{ \frac{1}{L^t} \sum_{j=1}^{N} f_j p_j^t : t = 1, \dots, T \right\} \right). \tag{13}$$

The minimization of this two-dimensional objective function is done by determining a dispatch that is optimal in a Pareto sense; see Section 5.1.

All the three problem variants have a demand constraint, balancing energy in a manner that the system load is met by generation of the set of available assets in the system. Since the latter sets change if a mechanism of demand response is put in place, so does the energy balance equation.

For the base case, the demand equation is

$$\sum_{j=1}^{N} p_j^t + \sum_{(m,k)} \sum_{i \in \mathcal{T}_k^m} \rho_i^t q_i^t = L^t - U^t,\ t = 1, \dots, T\,, \tag{14}$$

and the resulting problem is

$$\left\{ \begin{array}{ll} \min & J(p, z) \text{ in (13)} \\ \text{s. t.} & p_j \text{ satisfies (3), (4) for } j = 1, \dots, N \\ & (V, z, q) \text{ satisfy (7), (8)} \\ & (p, q) \text{ satisfy (14).} \end{array} \right. \tag{15}$$

When we consider the energy problem with load shaving, the amount of energy displaced at each time must be added to the power balance equation:

$$\sum_{j=1}^{N} p_j^t + \sum_{(m,k)} \sum_{i \in \mathcal{T}_k^m} \rho_i^t q_i^t + \delta^t = L^t - U^t,\ t = 1, \dots, T\,, \tag{16}$$

The bi-objective problem becomes

$$\left\{ \begin{array}{ll} \min & J(p, z) \text{ in (13)} \\ \text{s. t.} & p_j \text{ satisfies (3), (4) for } j = 1, \dots, N \\ & (V, z, q) \text{ satisfy (7), (8)} \\ & (\delta, v) \text{ satisfy (9)} \\ & (p, q, \delta) \text{ satisfy (16).} \end{array} \right. \tag{17}$$

Finally, when a battery energy storage system is considered, the energy that is injected in (b_I) or taken from

(b_O) the battery enters the power balance equation according to the following nonlinear relation:

$$b_O^t = -\min\left(0, \sum_{j=1}^{N} p_j^t + \sum_{(m,k)}\sum_{i\in\mathcal{T}_k^m} \rho_i^t q_i^t - L^t + U^t\right),$$
$$b_I^t = \max\left(0, \sum_{j=1}^{N} p_j^t + \sum_{(m,k)}\sum_{i\in\mathcal{T}_k^m} \rho_i^t q_i^t - L^t + U^t\right).$$

In words, when there is a surplus of energy, because there was more generation than demand, the surplus b_I^t is injected in the battery. Similarly, the battery will output the lacking energy b_O^t if there was not enough generation to satisfy the demand. The expressions above can be written in the form of constraints, as follows

$$\begin{aligned} &b_I^t \geq 0\,, b_O^t \geq 0, \text{ for all } t = 1,\dots,T,\\ &b_I^t \geq \sum_{j=1}^{N} p_j^t + \sum_{(m,k)}\sum_{i\in\mathcal{T}_k^m} \rho_i^t q_i^t - L^t + U^t,\\ &\qquad\qquad \text{for all } t = 1,\dots,T, \qquad (18)\\ &-b_O^t \leq \sum_{j=1}^{N} p_j^t + \sum_{(m,k)}\sum_{i\in\mathcal{T}_k^m} \rho_i^t q_i^t - L^t + U^T,\\ &\qquad\qquad \text{for all } t = 1,\dots,T, \end{aligned}$$

and the power balance equation has the expression

$$\sum_{j=1}^{N} p_j^t + \sum_{(m,k)}\sum_{i\in\mathcal{T}_k^m} \rho_i^t q_i^t + b_O^t - b_I^t = L^t - U^t,\ t = 1,\dots,T\,, \qquad (19)$$

The bi-objective problem becomes

$$\begin{cases} \min & J(p,z) \text{ in (13)}\\ \text{s. t.} & p_j \text{ satisfies (3), (4) for } j = 1,\dots,N\\ & (V,z,q) \text{ satisfy (7), (8)}\\ & (y, b_I, b_O) \text{ satisfy (10), (11), (12), (18)}\\ & (p,q,b_I,b_O) \text{ satisfy (19).} \end{cases} \qquad (20)$$

5. Multi-objective optimization

In the presence of more than one objective function, like (13), the meaning of a minimizer needs to be specified. We review below some concepts that are better understood in an abstract setting, that includes problems (15)-(20), and consider the problem

$$\begin{cases} \text{Minimize } & J(x) := (J_1(x), J_2(x))\\ \text{s. t. } & x \in X. \end{cases} \qquad (21)$$

For the results presented in this section, the functions can be arbitrary, in particular J_1 can be the sum of (1) and (5) and J_2 can have the expression (2). To exploit the max-structure of the latter objective, we write

$$J_2(x) = \max\left\{J_2^t(x) : t = 1,\dots,T\right\} \text{ with } J_2^t \text{ smooth}\,. \qquad (22)$$

Regarding the feasible set, for example (15) has decision variable is $x = (p, V, z, q)$ and set X gathering the constraints (3), (4) for $j = 1,\dots,N$, (7), (8), and (14).

5.1. Pareto solution and Pareto front

The wording "minimize" in (21) conveys the ambition of minimizing the two components of the objective function at the same time. Generally, this is not possible, and a compromise solution concept is given below:

- A vector $x^* \in X$ is a **weak Pareto solution** of (21) if there exist no $x \in X$, $x \neq x^*$ such that $J_i(x) < J_i(x^*)$ for all $i = 1, 2$. The set $\mathcal{P}_w$ of all weak Pareto optimal solutions is said to be weak Pareto optimal solutions set.
- A vector $x^* \in X$ is a **Pareto solution** of (21) if there exist no $x \in X$ such that $J(x) \neq J(x^*)$ and $J_i(x) \leq J_i(x^*)$ for all $i = 1, 2$. The set $\mathcal{P}$ of all Pareto optimal solutions is said to be Pareto optimal solutions set.

Clearly, the Pareto set is contained in the weak Pareto set: $\mathcal{P} \subset \mathcal{P}_w$. The set of all vectors of objective values at the Pareto (resp. weak Pareto) minima is said to be the *Pareto front* (resp. *weak Pareto front*).

In the following we discuss some methods to obtain (weak) Pareto optimal solutions. There are also methods that compute just one (weak) Pareto optimal solutions, but in this paper we look for methods to compute the entire Pareto front. Indeed if we could content ourselves with computing a single (weak) Pareto solution, then implicitly this would mean that we are capable of finding a desirable trade-off between both objectives. This amounts, in essence, to a mono-objective optimization problem, which is usually not the case, at least not for the application we have in mind. We assume it is important that all possible solutions are shown to the decision maker, who can then select the desired compromise, by choosing one point in the Pareto front.

5.2. Chebyshev Scalarization

A known approach for finding points in the Pareto front, called scalarization, defines a sequence of mono-objective optimization problems, in such a way that solutions to the multi-objective problem can be obtained

by solving instead a sequence of nonlinear programming problems. There is a large variety of methods for scalarizing a multi-objective optimization problem. The most popular scalarization function is defined as a weighted sum of the objective functions. Given a weight parameter $w \in [0,1]$, solving the mono-objective problem

$$\begin{array}{ll} \text{Minimize} & wJ_1(x) + (1-w)J_2(x) \\ \text{suject to:} & x \in X, \end{array} \tag{23}$$

leads to an optimal Pareto solution [6]. Since in our case, the objective J_2 is defined as a maximum of subfunctions $J_2^t,\ t = 1,\dots,T$, problem (23) would have a non smooth objective function that could be solved with the classical reformulation

$$\begin{array}{ll} \text{Minimize} & \alpha \\ \text{suject to:} & x \in X \\ & wJ_1(x) \le \alpha \\ & (1-w)J_2(x) \le \alpha. \end{array}$$

Another approach, called $\varepsilon-$constraint method, considers a mono-objective optimization problem with one component of the objective function taken as primary cost, and the other one transformed into a constraint, by setting an upper bound:

$$\begin{array}{l} \min\{J_2(x) \mid x \in X \quad \text{and } J_1(x) \le m_1, \quad m_1 \in \mathbb{R}\}, \\ \text{or} \\ \min\{J_1(x) \mid x \in X \quad \text{and } J_2(x) \le m_2, \quad m_2 \in \mathbb{R}\}. \end{array}$$

This method leads to a weak Pareto optimal solution [6].

We use a third alternative, called Chebyshev scalarization, see for instance [4–6]. When applied to (21), for a given weight $w \in [0,1]$, the method can be written as follows.

$$\begin{cases} \min & \max\left\{w(J_1(x)-\beta_1^*), (1-w)(J_2(x)-\beta_2^*)\right\} \\ \text{s.t.} & x \in X \end{cases} \tag{24}$$

where the parameters $\beta_i^*,\ i = 1,2$, are called *utopian* objective values. An utopian objective vector β^*, associated with a bi-objective problem, has components $\beta_i^* = z_i^* - \varepsilon_i$, where $\varepsilon_i > 0$ for $i = 1,2$ and z_i^* is the optimal value obtained when minimizing the objective function $J_i,\ i = 1,2$, individually, subject to the problem constraints. The following well-known theorem ensures that, among the weak Pareto solutions found by the Chebyshev scalarization when parsing the weight in the set $[0,1]$, one is in the Pareto front (not weak).

Theorem 1. *[6, Thm. 3.4.2 and 3.4.5]*

(i) The solution x^* of the weighted Chebyshev problem (24) *is weak Pareto optimal if all weighting coefficients are positive.*

(ii) Let x^* be Pareto optimal. Then there exists a weighting vector $w > 0$, such that x^* is a solution of weighted Chebyshev problem (24)*.*

Recall that in our application the feasible set is polyhedral, the first objective function is linear, and the second one is piecewise linear, so that problem (24) can be rewritten as follows:

$$\begin{cases} \min & \alpha \\ \text{s. t.} & x \in X \text{ and} \\ & w\left(J_1(x)-\beta_1^*\right) \le \alpha, \\ & (1-w)\left(J_2^t(x)-\beta_2^*\right) \le \alpha,\ t = 1,\dots,T\,. \end{cases} \tag{25}$$

As a result, for all the three instances considered in Section 4, namely (15), (17), and (20), the scalarized problem (25) is a linear programming problem, easily solved by a commercial solver.

The choice of a suitable range of values for w is fundamental to generate points in the Pareto front (not only weak solutions). To this end, we apply Algorithm 1, that solves the scalarized problem (25) for a sequence of suitably chosen parameters w, see Step 0.3 below.

Algorithm 1.

Step 0.0: (Initialization) *Choose the utopia parameters, $\varepsilon_1,\ \varepsilon_2 > 0$.*
Set the number of discrete (approximating) points, $N+1$, in the Pareto front. Set $k = 1$.

Step 0.1: (Front boundaries)
(a) Let x^1 minimize $J_1(x)$ over X.
Define $J_1^* = J_1(x^1)$ and $\bar{J}_2 = J_2(x^1)$.
Mark a boundary point in the Pareto front: $\bar{J}^N = (J_1^*, \bar{J}_2)$.
(b) Let x^2 minimize $J_2(x)$ over X.
Define $J_2^* = J_2(x^2)$ and $\bar{J}_1 = J_1(x^2)$.
Mark a boundary point in the Pareto front: $\bar{J}^0 = (\bar{J}_1, J_2^*)$.

Step 0.2: (Utopia point) *Set $\beta^* = (\beta_1^*, \beta_2^*)$ with $\beta_i^* = J_i^* - \varepsilon_i,\ i = 1,2$.*

Step 0.3: (Range of weights) *Set* $w_0 = \dfrac{(J_2^* - \beta_2^*)}{(\bar{J}_1 - \beta_1^*) + (J_2^* - \beta_2^*)}$ *and*

$$w_f = \frac{(\bar{J}_2 - \beta_2^*)}{(J_1^* - \beta_1^*) + (\bar{J}_2 - \beta_2^*)}.$$

Set the increment $\Delta w = (w_f - w_0)/N$.

Step k.1: (Current weight) *Set $w = w_0 + k\Delta w$.*

Step k.2: (Pareto point) *Find x^* solving problem* (25)*.*
Assign a point in the Pareto front: $\bar{J}^k = (J_1(x^*), J_2(x^*))$.

Step k.3: (Stopping criterion) *If $k = N$ then STOP.*
Otherwise, set k=k+1, and go to step k.1.

Algorithm 1 provides N points on the Pareto front, which in our setting gives points on a two-dimensional

curve, having the two objectives in the axes of the graph. Along the Pareto front, the obtained points represent acceptable trade-offs between operating economically the system and keeping low the system carbon emissions. The analysis below adds a third dimension to the curve, that can help the decision maker in choosing a specific trade-off.

5.3. Sensitivity analysis

In Linear Programming, shadow prices are Lagrange multipliers of certain constraint, giving the rate of change of the objective function when the constraint varies. We extend this sensitivity concept to the multi-objective setting, to determine how the variation of the first objective function affects the Pareto solution.

In mathematical terms, the aforementioned rate of change corresponds to the derivatives of certain perturbation function $v : \mathbb{R} \to \bar{\mathbb{R}}$. For our multi-objective problem, this is a nonsmooth function defined as:

$$v(r) = \min_{x \in X} \{J_2(x) \mid J_1(x) = r\} \ . \tag{26}$$

The optimality condition for the optimization problem in (26) writes down as

$$0 \in \partial J_2(x^*) + \pi_r \nabla J_1(x^*) + \nu^*, \tag{27}$$

for some multiplier $\pi_r \in \mathbb{R}$ and a normal element

$$\nu^* \in N_X(x^*) = \left\{ g \in \mathbb{R}^n \mid \ g^\top (y - x^*) \leq 0, \ y \in X \right\}.$$

The multiplier and normal element exist, thanks to our assumption that J_1 is linear (1), J_2 is piecewise linear (2), and X is polyhedral.

Moreover, by [20, Chapter VII, Thm 3.3.2], it holds that $-\pi_r \in \partial v(r)$, so the multiplier is indeed a shadow price in (26). In terms of our multi-objective setting, $-\pi_r$ describes how the second objective changes ($v(r) = J_2(x^*)$), when the first objective varies ($r = J_1(x^*)$).

Theorem 2 shows how to compute such shadow price directly from the primal-dual solution of the Chebyshev scalarization (25) for a given w, *without solving an additional optimization problem* (26).

Theorem 2. *Given $w \in (0, 1)$, consider* (25)*, with J_2 given as a max-function of the form* (22)*. At Step k.2 of Algorithm 1 a Pareto point x^*_w, solving problem* (25)*, is computed, together with the optimal value α^*_w, normal element $\nu^* \in N_X(x^*_w)$, and μ^*_1, the Lagrange multiplier associated with the constraint $w\left(J_1(x) - \beta^*_1\right) \leq \alpha$.*

If $\mu^*_1 \neq 0$ and $\mu^*_1 \neq 1$, then x^*_w satisfies the optimality condition (27)*, written with ν^* and*

$$\begin{aligned} \textit{perturbation} \quad r &= \beta^*_1 + \frac{\alpha^*_w}{w}, \textit{and} \\ \textit{shadow price} \quad \pi_r &= \frac{\mu^*_1 w}{(1-\mu^*_1)(1-w)}. \end{aligned}$$

PROOF. If the pair (x^*_w, α^*_w) solves problem (25), there exist multipliers $\mu^*_1,\ \mu^*_{2,t} \geq 0,\ t = 1, \ldots, T$ and a normal element $\nu^* \in N_X(x^*)$, such that

$$\begin{pmatrix} 1 - \mu^*_1 - \sum_{t=1}^T \mu^*_{2,t} \\ w\mu^*_1 \nabla J_1(x^*) + (1-w) \sum_{t=1}^T \mu^*_{2,t} \nabla J^t_2(x^*) + \nu^* \end{pmatrix} = 0, \tag{28}$$

$$\mu^*_1 (w\,(J_1(x^*) - \beta^*_1) - \alpha^*) = 0, \tag{29}$$

$$\mu^*_{2,t}((1-w)\,(J^t_2(x^*) - \beta^*_2) - \alpha^*) = 0, \quad \text{for t=1,...,T} \tag{30}$$

By equation (29), it must be that either $\mu^*_1 = 0$ or $w\left(J_1(x^*) - \beta^*_1\right) - \alpha^* = 0$. By assumption, $\mu^*_1 \neq 0$, so $J_1(x^*) = \beta^*_1 - \dfrac{\alpha^*}{w}$.

Because of (22), the subdifferential in (27) is

$$\partial J_2(x^*) = conv\{\nabla J^t_2(x^*) : t = 1, ..., T \text{ s.t. } J^t_2(x^*) = J_2(x^*)\}.$$

By (30), we obtain that $J^t_2(x^*) = \beta^*_2 - \dfrac{\alpha^*}{1-w}$ if and only if $\mu^*_{2,t} \neq 0$. By (28), we have $1 - \mu^*_1 = \sum_{t=1}^T \mu^*_{2,t}$. This, together with $\mu^*_{2,t} \neq 0$ and the assumption that $1 - \mu^*_1 \neq 0$, is equivalent to the existence of at least one $t \in \{1, \ldots, T\}$ with $\mu^*_{2,t} \neq 0$. We conclude that $\displaystyle\sum_{t=1}^T \frac{\mu^*_{2,t}}{\sum_{t=1}^T \mu^*_{2,t}} = 1$ and consequently:

$$G := \sum_{i=1}^T \frac{\mu^*_{2,t}}{\sum_{t=1}^T \mu^*_{2,t}} \nabla J^t_2(x^*) \in \partial J_2(x^*).$$

Altogether we have proved the identity

$$G + \frac{w\mu^*_1}{(1-\mu^*_1)(1-w)} \nabla J_1(x^*) + \nu =^* 0,$$

showing that x^* satisfies (27), as stated. □

The assumption on μ^*_1 ensures that the shadow price is not zero and well defined. The meaning of the assumption is understood when interpreting the multiplier in terms of the optimality condition of problem (24). Namely, because the objective function therein is a max-function, there exists $\mu^*_1 \in [0, 1]$ such that the optimal value in (24) is equal to

$$\mu^*_1 w(J_1(x^*) - \beta^*_1) + (1 - \mu^*_1)(1 - w)(J_2(x^*) - \beta^*_2)\,,$$

and

$$0 = \mu_1^* w J_1'(x^*) + (1-\mu_1^*)(1-w) g_2^* + \nu^* \text{ for } g_2^* \in \partial J_2(x^*)\,.$$

The cases $\mu_1^* = 0$ or $\mu_1^* = 1$ correspond to (the undesirable situation of) the scalarization resulting in the minimization of only one objective. For instance, setting $\mu_1^* = 1$ in the relations above implies that the problem

$$\min w(J_1(x) - \beta_1^*) \text{ s.t. } x \in X$$

is equivalent to problem (24). As a result, the assumptions of Theorem 2 are natural in the considered setting.

6. Numerical results

The three problem variants, (15)-(20), are benchmarked on a set of three stylized systems, representing configurations typical in Brazil, France and Germany. As mentioned, the respective composition of the power mix is mostly hydro, balanced between thermal and hydro, and mostly thermal. Since the second objective control carbon emissions of the thermal power plants, we expect the impact of the environmental objective to higher in the thermally-dominated German-like system.

The code was written in MATLAB and run on a Samsung, Intel(R) Core(TM) i7-7500U, CPU 2.70GHz, com 8GB RAM, 64-bit. Algorithm 1 was run with $N = 100$ for the Brazilian and French systems and $N = 200$ for Germany. At Step k.2, since all the scalarized problem (25) are linear programs, the built-in solver *linprog* was used.

6.1. Data common to all the systems

The carbon emission rate f in kilogram per megawatt-hour (Kg/MWh) is considered constant over time. The considered values, the same for all the instances, relate to each type of technology and are given in Table 1.

Thermal units	CO2 emission (Kg/MWh)
Nuclear	0
Lignite	1140
Coal	940
Gas	570
Mineral oil	770
Biomass	770
Combustion turbine	1200

Table 1: Carbon emission by type of thermal unit

The solar generation for the whole period is represented in Figure 1.

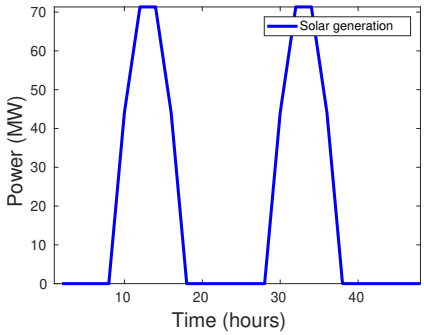

Figure 1: Solar generation on a cold sunny winter day.

In problem (17), the load shaving mechanism can displace power up to a maximum $\gamma = 100$ MW. For the batteries in (20), we consider three batteries, with different input and output, as well as different maximum capacity, see Tables 2 and 3.

	Q_B	b_I^{max}	b_O^{max}
Battery 1	117 MWh	13.2 MW	40 MW
Battery 2	234 MWh	26.4 MW	80 MW
Battery 3	400 MWh	100 MW	100 MW

Table 2: Battery sizes.

y^{min}	0.1
y^{max}	1
ρ_I	0.95
ρ_O	0.95
y^0	0.5

Table 3: Battery data, the same for sizes.

Both the Brazilian and French configurations use the configuration for load displacement and batteries given above. The same data is multiplied by a factor of 20 for the German case, scaling the input proportionally to the system larger size; see Table 12.

6.2. Hydro-dominated Brazilian system

The Brazilian instance represents schematically the main subsystems in the country, each one synthesized in a single bus. Each bus has its own demand to meet, but it is interconnected with some other buses and can exchange energy with other nodes; see Figure 2.

The transmission system has 5 buses and 6 lines, whose transmission capacity is 1.000 MW and reactance $0,0249$ pu, with the exception of line $2-5$, which has a capacity of 2.000 MW and reactance $0,0124$ pu.

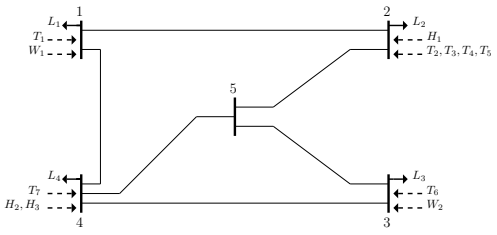

Figure 2: Diagrammatic representation of the Brazilian system

The representation of the transmission system is an important modeling issue, since the capacity of transmission lines has an impact on the generation profiles. Based on [21], in this work a classical DC (direct current) model is employed, assuming that

- all bus voltages are fixed an equal to 1 p.u.;
- line resistances are negligible compared to line reactances; and
- angle (θ) differences between buses are small, so that $\sin(\theta) \approx \theta$ in radians.

With these assumptions, the power flow in each transmission line can be modelled by linear constraints [22]. The corresponding line limits and power balance equations are

$$-FL_l^{max} \leq \sum_{b=1}^{B} \Gamma_{lb}\Big(\sum_{j \in T_b} p_j^t + \sum_{i \in H_b} \rho_i^t q_i^t + W_b^t - L_b^t \Big) \leq FL_l^{max}$$

$$\sum_{b=1}^{B} \Big(\sum_{j \in T_b} p_j^t + \sum_{i \in H_b} \rho_i^t q_i^t + W_b^t \Big) = \sum_{b=1}^{B} L_b^t,$$

for $t = 1, \ldots, T$, where B is the number of buses, T_b is the set of thermal units connected to bus b, H_b is the set of hydro plants connected to bus b, $\rho_i q_i$ is the output power of hydro plant i, W_b^t represents the wind energy generated by bus b at time step t, L_b^t is the load demand of bus b ate time step t, FL_l^{max} is the maximum power flow capacity of the transmission line l (MW). The power transfer distribution factor of transmission line l due to the injection of active power at bus b, Γ_{lb}, depends on the reactance of the transmissions lines and represents the sensitivity of each power injection at bus b over line l. This parameter is obtained through manipulations on equations of power flow, power balance on buses and the incidence matrix as described in [23].

The system is composed of seven thermal units ($T_1 - T_7$), three hydro plants ($H_1 - H_3$) and two wind units ($W_1 - W_2$). We consider the time horizon T to span 24 hours and with time step size h equal to 1 hour.

The thermal unit data is given in Table 4 below of three different types: 2 gas ($T_1 - T_2$), 3 mineral oil ($T_3 - T_5$), 1 coal (T_6) and 1 biomass (T_7).

Thermal units	Bus	p^0	p^{max}	θ	c_j
T_1	1	0	455	75	15
T_2	2	0	160	70	20
T_3	2	0	80	30	50
T_4	2	0	55	15	60
T_5	2	0	55	15	80
T_6	3	200	455	100	35
T_7	4	0	130	40	25

Table 4: Thermal unit data for the Brazilian system

Table (5) has the data related to the hydro plants. The first power plant, H_1, consists of three, while $H2$ and $H3$ consist of five and four identical units, respectively. The volumes are given in hm^3, the maximum flow rate of each turbine in h^3/s and the cost of the water c_w in Brazilian Real (R$). Reservoir H_3 is downstream with respect to H_2 with travel time equal to one hour. Reservoir H_1 is uphill with respect to H_2 and there is no water delay between both reservoirs.

Plant	Bus	V^{min}	V^{max}	V_0	q^{max}	c_w
H_1	2	1974	5776	2000	344	50
H_2	4	2283	3340	2500	437	50
H_3	4	4300	5100	4500	318	50

Table 5: Hydro- plant data Brazilian system

The demand to be met is located in four load centers ($L_1 - L_4$). Bus 5 is considered to be the slack bus, i.e., it does not have a demand to meet. The demand for each bus and the wind generation of units W_1 and W_2 are given in Figure 3.

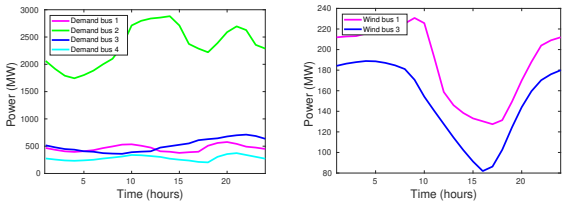

Figure 3: Demand and wind generation for the Brazilian system (left and right)

The battery and the load shaving mechanism are attached to bus 4, with the largest generation capacity.

Figure 4 shows the Pareto front, with black dots indicating the optimal value obtained for each one of the two objectives problem with $w = 0.9$.

By examining the Pareto front, the option that reduces the most both the cost and the carbon emission is battery

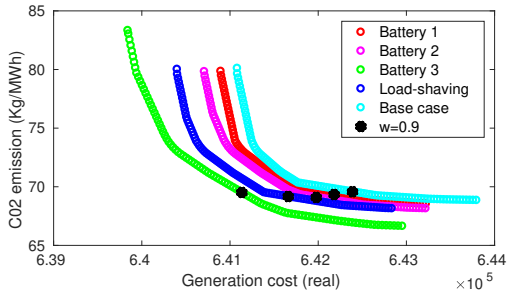

Figure 4: Pareto front for the Brazilian system

3, that is the largest battery. Load shaving is a mechanism better than batteries 1 and 2 in this configuration: in a hydro-dominated system, it takes a large battery to have the same effect. A possible justification is given by the transmission system, which adds more constraints to the feasible set, and in particular, contrains the exchanges of energy to be within the line limits. Hence, it is necessary to dispose of a larger battery to obtain better results than the load-shaving (which by nature can be diffuse).

Table 6 shows the final value of the two objectives when w equal 1, 0, and 0.9, respectively. Recall from equation (25) that the parameter w defines the scalarization; specifically, when $w = 1$ (respectively $w = 0$) only the operating cost (respectively the maximum CO_2 emission) is considered. For each value of w, a first row reports the operating cost and the maximum CO_2 emission for the base case. The gains in both objectives, absolute and percentage magnitudes, are displayed subsequently, for the model (17) with load shaving, and for the model (20), using the three battery configurations in Table 2.

		Cost	%	CO_2	%
$w = 1$	Base case	641.083,00	-	80.10	-
	Load shaving	-682,00	-0.11 %	-0.08	-0.1 %
	Battery 1	-187,00	- 0.03 %	-0.25	-0.31 %
	Battery 2	-374,00	-0.06 %	-0.27	-0.34 %
	Battery 3	-1.241,00	-0.19 %	+3.23	+4.03 %
$w = 0$	Base case	643.795,00	-	68.85	-
	Load shaving	-960,00	-0.15%	-0.70	-1.03 %
	Battery 1	-571,00	-0.09 %	-0.30	-0.44%
	Battery 2	-575,00	-0.09%	-0.70	-1.03 %
	Battery 3	-840,00	-0.13 %	-2.21	-3.21 %
$w = 0.9$	Base case	642.389,00	-	69.75	-
	Load shaving	-729,00	-0.11%	-0.41	-0.59 %
	Battery 1	-209,00	-0.03 %	-0.20	-0.34%
	Battery 2	-411,00	-0.06%	-0.48	-0.68 %
	Battery 3	-1.255,00	-0.19%	-0.06	-0.08 %

Table 6: Generation cost and CO_2 emission for Brazilian system

Results with $w = 1$ and $w = 0$ correspond, respectively, to a "purely operational" and a "fully green" decision maker. Somewhat contrary to the first intuition, when $w = 1$, the largest battery, number 3, results in an increase of CO_2 emissions. We conjecture this is because the result of storing energy from some thermal units with generation cost lower than the price of the water. In all the instances, generation costs are reduced with respect to the base case, even when $w = 0$ and minimizing operating cost is not an objective.

The case $w = 0.9$ represents a plausible scenario for an independent operator of a hydro-dominated system like the one under consideration. In such circumstances, the operator is naturally more concerned by reducing operating costs than by reducing the system emissions ($1 - w = 0.1$), simply because the carbon footprint of the mix is already low.

6.3. Balanced Hydro-Thermal French system

The time horizon T spans 48 hours, with time step size h of 2 hours. There are no transmission lines in this configuration.

The system has 9 thermal units, of 4 different types: 3 nuclear (T_1-T_3), 2 coal (T_4-T_5), 3 gas (T_6-T_8) and 1 combustion turbine (T_9); see Table 7 below. The operating cost c_j, in euro per megawatt-hour (€/MWh) is constant.

Thermal units	p^0	p^{max}	θ	c_j
T_1	750	900	100	30
T_2	750	900	100	35
T_3	750	900	100	37
T_4	75	300	30	45
T_5	75	300	30	55
T_6	0	200	20	60
T_7	0	200	20	100
T_8	0	200	20	110
T_9	0	150	10	150

Table 7: Thermal unit data

Hydraulic electricity is generated by plants in cascade along two hydro-valleys, called Ain and Isère, whose hydraulic configuration is given in Figure 5 and whose data is reported in Tables 8 and 9. All turbines of each power plant are considered identical, but each plant has a varying number of turbines. The volumes are given in hm^3, the maximum flow rate of each turbine q^{max} in m^3/s and the cost of the water c_w in euros.

In problems (17) and (20), the respective load shaving and battery data is the same than for the Brazilian system.

The French configuration has no wind. The demand for the whole period is shown in Figure 6.

In Figure 7, with the Pareto Front, black dots indicate the optimal value obtained for each one of the two

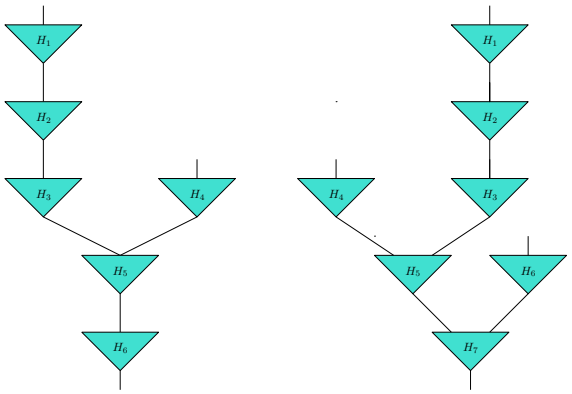

(a) Ain valley (b) Isère valley

Figure 5: French hydro-valleys.

Plant	Turbines	V^{min}	V^{max}	V_0	q^{max}	c_w
H_1	4	150	417.80	277.50	72.5	40
H_2	2	0.96	1.5	1.011	100	35
H_3	2	33.27	35.12	34.38	120	30
H_4	2	0.88	4.38	1.84	15	33
H_5	3	10.81	13.59	12.9	60	28
H_6	3	17.6	18.2	18.1	90	25

Table 8: Hydro-plant data in Ain valley

Plant	Turbines	V^{min}	V^{max}	V_0	q^{max}	c_w
H_1	3	4	9.78	5	11	35
H_2	3	3	223.83	133.43	16	40
H_3	4	0	0.1	0.05	10	30
H_4	2	0	0.1	0.05	12	33
H_5	3	0.1	0.6	0.3	3.3	28
H_6	4	0.1	1.32	0.5	47.7	35
H_7	4	0.09	0.3	0.1	25	25

Table 9: Hydro-plant data in Isère valley

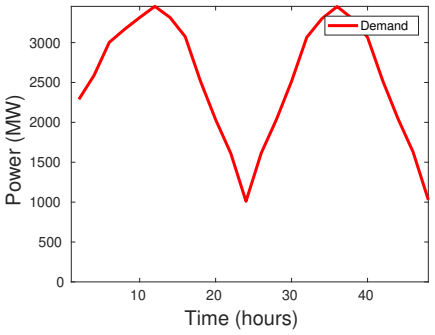

Figure 6: Demand on a cold sunny winter day for the French system.

objectives problem with $w = 0.5$, that is, when both objectives have the same weight in the scalarization. This is a sound criterion when operating a balanced system, as the one under consideration.

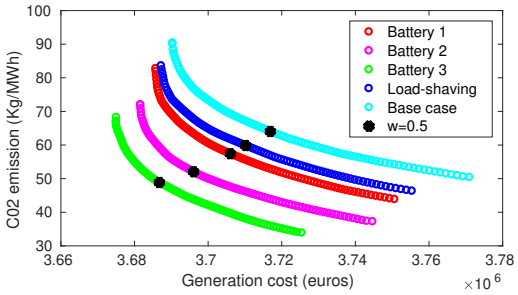

Figure 7: Pareto front for French system

Once more, the option that reduces the most the operating cost and the carbon emission, simultaneously, is the largest battery 3. Load shaving is an efficient mechanism, comparable to battery 1.

Table 10 reports the final value of the two objectives, discriminating the percentage of improvement for all the instances and when w equal 1, 0, and 0.5.

		Cost	%	CO_2	%
$w = 1$	Base case	3.690.352,00	-	90,41	-
	Load shaving	-3.100,00	-0.08 %	-6.82	-7.55 %
	Battery 1	-4.581,00	- 0.12 %	-7.14	-7.89 %
	Battery 2	-8.720,00	-0.24 %	-17.23	-19.05 %
	Battery 3	-15.320,00	-0.41 %	-22.16	-24.51 %
$w = 0$	Base case	3.770.995,00	-	50.38	-
	Load shaving	-15.632,00	-0.41%	-4.06	-8.07 %
	Battery 1	-20.363,00	-0.54 %	-6.54	-12.97%
	Battery 2	-26.335,00	-0.70%	-13.15	-26.10 %
	Battery 3	-45.581,00	-1.21 %	-16.49	-32.74 %
$w = 0,5$	Base case	3.716.891,00	-	64.05	-
	Load shaving	-6.684,00	-0.18%	-4.22	-6.59 %
	Battery 1	-10.828,00	-0.29 %	-6.64	-10.37%
	Battery 2	-20.841,00	-0.56%	-12.01	-18.76 %
	Battery 3	-30.140,00	-0.81%	-15.19	-23.72 %

Table 10: Generation cost and CO_2 emission French system

The figures in Table 10 show an improvement with respect to the base case, both in operating cost and CO_2 emissions. Notably, even with $w = 1$ (CO_2 emissions are not taken into account in the objective), the mechanisms for moving energy in time contribute to reducing the fuel emissions! If the same weight is assigned to the two objective functions, i.e., $w = 0.5$, we notice a better control over the total emissions, with respect to $w = 1$. In the realistic setting, $w = 0.5$, battery 3 reduces operating cost and cuts down carbon emissions in more than 20%.

The comparison of the figures in the last column of Tables 6 and 10 is revealing. For the Brazilian case, the best percentage of CO_2 reduction brought by the energy management tools is -3.21 (battery 3, $w = 0$). By contrast, in the French system, with more thermal gen-

eration, the reduction is much more significant, more than 10 times larger (-32.74, battery 3, $w = 0$).

A final illustration of the system operation is given in Figure 8, with the dynamics of battery 3 and the load shaving mechanism along the planning time.

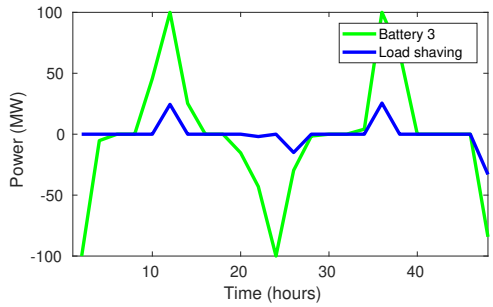

Figure 8: Battery 3 profile and load shaving for $w = 0.5$ for the French system

Positive profile values mean discharged energy, the battery output, while negative values represent stored energy stored, the battery input. As expected, the batteries provide energy to the system at peak times, and get replenished when demand is low. Similarly for with load shaving, but to a lesser extent.

6.4. Thermally Dominated German system

The system has six thermal units, one run-of-the-river hydro-power plant, one solar and one wind plant, and no transmission network.

The operating cost c_j in euro per megawatt-hour (€/MWh) is constant over time. Each thermal unit is of a different type: nuclear, brown coal (lignite), hard coal, gas, mineral oil and biomass; see Table 11 below.

Thermal units	p^0	p^{max}	θ	c_j
T_1	9329	9516	1057	35
T_2	14551	19989.3	1999	45
T_3	1946	22699.6	2270	55
T_4	1626	24434.7	2443	90
T_5	191	2614.7	175	150
T_6	4489	7320.1	732	40

Table 11: German's thermal unit data

The time horizon and time step are identical to those for the French case.

In problem (17), the load shaving mechanism can displace power up to a maximum $\gamma = 2000$ MW. Battery data is as shown in Table 3 with maximum capacity, output and input power as in Table 12.

With respect to the data for France, it was multiplied by a factor of 20 because the system demand is around 20 times larger than in the French system. After scaling, the total load shifting capacity is around 2% of peak consumption, an appropriate order of magnitude when considering thermostatic load shifting potential.

	Q_B	b_I^{max}	b_O^{max}
Battery 1	2340 MWh	264 MW	800 MW
Battery 2	4680 MWh	328 MW	1600 MW
Battery 3	8000 MWh	2000 MW	2000 MW

Table 12: Battery data for German system

The demand, solar, wind, and run-of-the-river generation for the whole period are given in Figure 9.

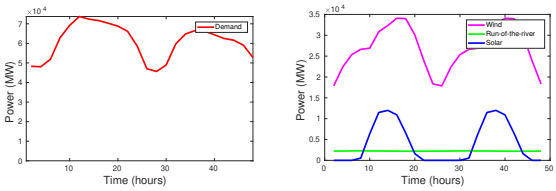

Figure 9: Demand and solar, wind and run-of-the-river generation of a spring German day

The Pareto front in Figure 10 shows the result for the given demand, in a spring day. As with the two other systems, the option that reduces the most both the operating cost and the carbon emission is battery 3. The efficiency of load shaving remains comparable to the smallest battery 1.

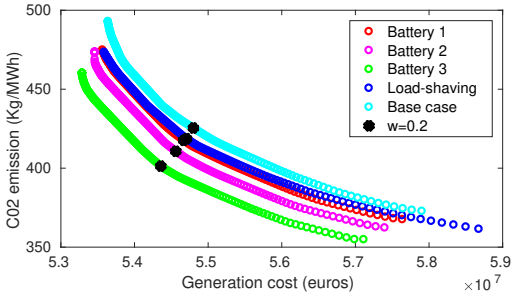

Figure 10: Pareto front for German system

Table 13 shows the final value of the two objectives when the parameter w is equal 1, 0 and 0.2, respectively. The last value is sound for a mix with high proportion of thermal power, since $1 - w = 0.8$ is the weight given in the scalarization (25) to the control of carbon emissions, via the second objective, (2).

In the German configuration, the mechanism of load shaving results in a cost increase when $w = 0$, for a purely green operator. The carbon emissions are reduced in all the instances and battery 3 gives the best

		Cost	%	CO_2	%
$w = 1$	Base case	53.640.087,00	-	492.94	-
	Load shaving	-58.865,00	-0.11 %	-18.60	-3.77 %
	Battery 1	-98.132,00	- 0.18 %	-15.32	-3.11 %
	Battery 2	-176.792,00	-0.33 %	-10.18	-2.06 %
	Battery 3	-348.998,00	-0.65 %	-15.69	-3.18 %
$w = 0$	Base case	57.903.467,00	-	372.77	-
	Load shaving	+975.380,00	+1.68%	-11.88	-3.17 %
	Battery 1	-264.926,00	-0.46 %	-5.25	-1.41%
	Battery 2	-504.849,00	-0.87%	-10.50	-2.81 %
	Battery 3	-789.857,00	-1.36 %	-17.94	-4.81 %
$w = 0.2$	Base case	54.798.647,00	-	425.42	-
	Load shaving	-89.702,00	-0.16%	-6.82	-1.68 %
	Battery 1	-130.522,00	-0.24 %	-7.76	-1.82%
	Battery 2	-237.123,00	-0.43%	-14.69	-3.45 %
	Battery 3	-441.068,00	-0.80%	-24.10	-5.67 %

Table 13: Generation cost and CO_2 emission for German system

improvement. When comparing the percentages of reduction with the ones obtained with the French system, we observe that the numbers are less significant, like in the Brazilian system. The reason is clear: in a diversified power mix, more balanced, like the French one, there are synergies that can be exploited in order to reduce both operating costs and carbon emissions.

Figure 11 shows the dynamics of battery 3 and load shaving for $w = 0.2$.

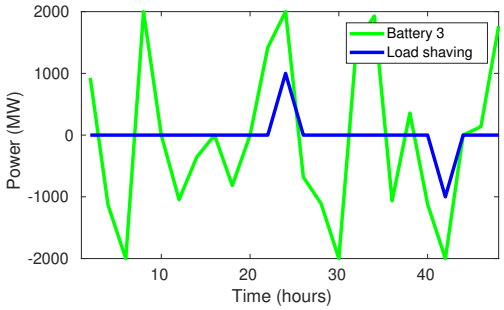

Figure 11: Battery 3 profile and load shaving for $w = 0.2$ for the German system.

Differently from Figure 8, the battery is not used only at peak times like the load-shaving, but several times during the day. The energy neutral shift modelling (the bottom equality in (9)) makes the load-shaving mechanism less flexible than the battery, which can input and output energy without such constraints.

6.5. Three-dimensional Pareto graphs

The sensitivity of the second objective (maximum emissions) with respect to the operating cost, given by Theorem 2 is presented in Figures 12-14 for the three systems.

The value is negative, as the CO_2 emissions decrease when the generation cost increases, and has a similar behaviour for all the configurations. Moreover, it is possible to see that the rate of change decreases when the generation cost gets further away from the value obtained when minimizing only the maximum carbon emissions ($w = 0$). On the other side, when closer to the optimal value of minimizing just the operating cost ($w = 1$), a small increase in the generation costs yields a large reduction of the CO_2 emission.

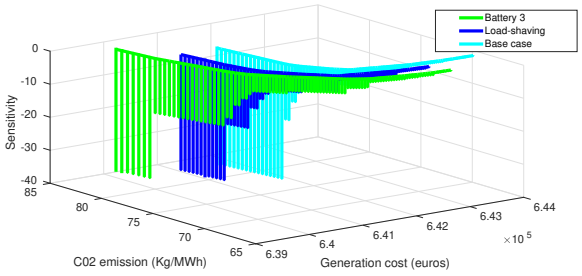

Figure 12: Sensitivity of the CO_2 emission with respect to the operating cost for the Brazilian system

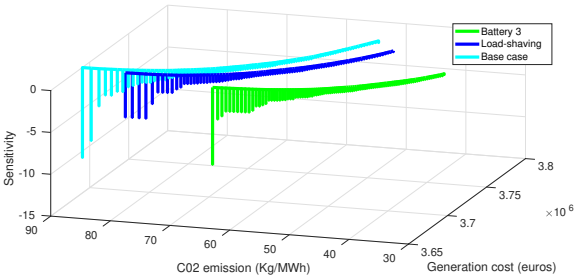

Figure 13: Sensitivity of the CO_2 emission with respect to the operating cost for the French system

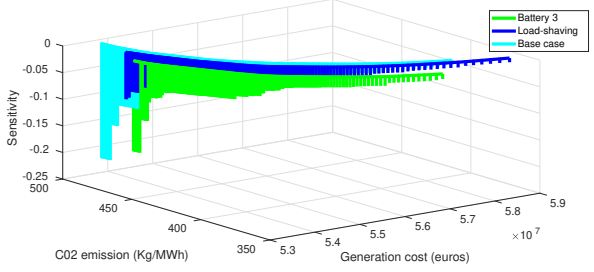

Figure 14: Sensitivity of the CO_2 emission with respect to the operating cost for German system

7. Conclusions

In this work we studied the effect of different batteries, and a load shaving mechanism on bi-objective energy management problems. The first objective consists in controlling cost, whereas the second consists of controlling carbon emissions. The study was carried out on simple, yet representative, mixes for power systems: thermal dominated, hydro dominated, hydro-thermal system. Both mechanisms, load shaving and battery provide a reduction in operating cost and carbon emissions. Moreover, if the battery is sufficiently large, the results are better than with load shaving. The size of the required battery was shown to depend on modelling transmission system constraints. In our study, demand-side management provides good results, in general comparable to the case with the smaller battery. Since the former does not require the installation of costly physical material, demand-side management may prove quite valuable. However, batteries are more flexible and can be preferable for smoothing profiles not only at peaks.

The presented bi-objective approach can be extended to consider larger and more realistic models. We have also given a sensitivity analysis that provides useful information to the decision maker when choosing a compromise between conflicting objectives.

Acknowledgements

We thank Guilherme Matiussi-Ramalho and Erlon Cristian Finardi for the Brazilian data, and Daniel Beulertz for the German data.

C. Sagastizábal thanks the Isaac Newton Institute for Mathematical Sciences for support and hospitality during the programme *The Mathematics of Energy Systems* when work on this paper was undertaken. This work was supported by: EPSRC grant number EP/R014604/1. The authors gratefully acknowledge support by the Fondation Mathématique Jacques Hadamard through the Program Gaspard Monge in optimization and operations research.

References

[1] https://www.lemondedelenergie.com/europe-blackout-electricite/2019/01/17/.

[2] M. Pereira, L. Pinto, Multi-stage stochastic optimization applied to energy planning, Math. Program. 52 (2) (1991) 359–375 (1991).

[3] A. Chaouachi, R. M. Kamel, R. Andoulski, K. Nagasaka., Multiobjective intelligent energy management for a microgrid, IEEE Trans. on Industrial Electronics 4 (60) (2013) 1688–1699 (2013).

[4] J. Jahn, Vector optimization: theory, applications and extensions, Springer, Berlin, 2011 (2011).

[5] C. Y. Kaya, H. Maurer, A numerical method for nonconvex multi-objective optimal control problems, Computational Optimization and Applications 57 (3) (2014) 685–702 (2014).

[6] K. Miettinen, Nonlinear multiobjective optimization, Kluwer Academic, Norwell, 1999 (1999).

[7] M. Tahanan, W. van Ackooij, A. Frangioni, F. Lacalandra, Large-scale unit commitment under uncertainty: a literature survey, 4OR 13 (2) (2015) 115–171 (2015). doi:10.1007/s10288-014-0279-y.

[8] W. van Ackooij, I. Danti Lopez, A. Frangioni, F. Lacalandra, M. Tahanan, Large-scale unit commitment under uncertainty: an updated literature survey, Annals of Operations Research 271 (1) (2018) 11–85 (2018).

[9] R. Taktak, C. d'Ambrosio, An overview on mathematical programming approaches for the deterministic unit commitment problem in hydro valleys, Energy Systems 8 (1) (2017) 57–79 (2017). doi:10.1007/s12667-015-0189-x.

[10] W. van Ackooij, R. Henrion, A. Möller, R. Zorgati, Joint chance constrained programming for hydro reservoir management, Optimization and Engineering 15 (2014) 509–531 (2014).

[11] M. Uddin, M. F. Romlie, M. F. Abdullah, S. A. Halim, A. H. A. Bakar, T. C. Kwang, A review on peak load shaving strategies, Renewable and Sustainable Energy Reviews 3 (82) (2018) 3323–3332 (2018).

[12] D. Javor, A. Janjic, Application of demand side management techniques in successive optimization procedures, Communications in dependability and Quality Management, An International Journal 4 (19) (2016) 40–51 (2016).

[13] G. Strbac, Demand side management: Benefits and challenges, Energy Policy 36 (12) (2008) 4419–4426 (2008).

[14] M. Negnevitsky, K. Wong, Demand-side management evaluation tool, IEEE Transactions on Power Systems 1 (30) (2015) 212–222 (2015).

[15] J. Leadbetter, L. G. Swan, Selection of battery technology to support grid-integrated renewable electricity, Journal of Power Sources 216 (2012) 376–386 (2012).

[16] A. Rahimi, M. Zarghami, M. Vaziri, S. Vadhva, A simple and effective approach for peak load shaving using battery storage systems, North American Power Symposium (NAPS) (2013) 1–5 (2013).

[17] Y. Xu, C. Singh, Multi-objective design of energy storage in distribution systems based on modified particle swarm optimization, IEEE Power and Energy Society General Meeting (2012) 1–8 (2012).

[18] E. Telaretti, L. Dusonchet, Battery storage systems for peak load shaving applications: Part 1: Operating strategy and modification of the power diagram, IEEE International Conference on Environment and Electrical Engineering (EEEIC) (2016) 1–6 (2016).

[19] B. Heymann, P. Martinon, F. Silva, F. Lanas, G. Jiménez, J. Bonnans, Continuous optimal control approaches to microgrid energy management, Online first (2017).

[20] J.-B. Hiriart-Urruty, C. Lemaréchal, Convex Analysis and Minimization Algorithms I, Springer-Verlag, New York, 1993 (1993).

[21] M. R. Scuzziato, Modelo de otimização estocástica de dois estágios para o problema da programação diá ria da operação eletroenergética, Ph.D. thesis, Universidade Federal de Santa Catarina, Brasil, in Portuguese (2016).

[22] C.-L. Tseng, S. S. Oren, C. S. Cheng, C. Li, A. J. Svoboda, R. B. Johnson, A transmission-constrained unit commitment method in power system scheduling, Decision Support Systems 24 (3-4) (1999) 297–310 (1999).

[23] K. Van Den Bergh, E. Delaure, W. D'Haeseller, DC power flow in unit commitment models, KU Leuven Energy Institute (2014).